AIAA JOURNAL
Vol. 35, No. 10, October 1997

Technical Notes

TECHNICAL NOTES are short manuscripts describing new developments or important results of a preliminary nature. These Notes cannot exceed 6 manuscript pages and 3 figures; a page of text may be substituted for a figure and vice versa. After informal review by the editors, they may be published within a few months of the date of receipt. Style requirements are the same as for regular contributions (see inside back cover).

Three-Dimensional Instability of a Pair of Trailing Vortices near the Ground

N. V. Kornev* and G. Reichert†
Technical University of Brunswick, 38023 Brunswick, Germany

Introduction

THE vortex behavior near the ground is a very important scientific problem for many reasons.[1,2] Dee and Nicholas[3] and Harvey and Perry[4] seem to be the first to have published an experimental study of the vortex behavior near the ground, including the vortex rebound phenomenon. Van Heijst and Flor[5] studied the vortex–wall encounters in stratified flow. Barker and Crow[6] simulated the vortex rebounding near the water-free surface in a water tank. Ciffone and Pedley[7] made detailed measurements of the trailing vortex trajectory and velocity field in lift-generated wakes.

The important theoretical contribution to the study of the vortex–wall interactions was made by the authors who used the interacting boundary-layer formulations.[2] Thanks to the rapid development of computers, the direct numerical study of vortex–wall interaction by means of finite difference solutions of the full Navier–Stokes equations has become possible in the past few years. Several numerical models and results of calculations have been published with various motivations, ranging from fundamental physics to engineering application.[8–10] Teske et al.[11] developed an approximate model to predict the decay of aircraft vortices due to the atmospheric effects at a large height above the ground.

Most of the numerical simulations were carried out using two-dimensional formulations. Three-dimensional instability of the trailing vortex near the ground has been unexplored. The experimental observations were made under some ideal conditions without accounting for the unsteady loading of the vortex-generating aircraft and the strong turbulence effects. Now it is well known that the three-dimensional sinusoidal vortex instability called Crow instability plays a key role in the aircraft vortex decay. The first analytical study of the sinusoidal instability in a pair of counter-rotating vortex tubes shed from the wing tips of an airplane was carried out by Crow.[12] Bliss[13] and Crow and Bate[14] have applied the Crow stability theory to predict the time of vortex decay. Green[15] and Liu[16] have investigated the atmospheric conditions under which Crow instability is dominant.

The current analytical and numerical study has concentrated on the investigation of the three-dimensional trailing vortex instability near the ground. The vortex roll-up process is assumed to be complete, and two trailing counter-rotating vortices are considered. We propose an extension of the Crow stability theory on the ground effect. We found three types of vortex instability, depending on the dimensionless height of initial position $H = h/b$ of the trailing vortices.

Received Nov. 12, 1996; revision received May 8, 1997; accepted for publication May 19, 1997.

*Humboldt Stipendiat; currently Associate Professor, Department of Hydromechanics, Marine Technical University, Lotsmanskaya 3, 190008 St. Petersburg, Russia. E-mail: kornev@mtu-ic.spb.su.

†Professor, Institute of Flight Mechanics. Senior Member AIAA. Deceased.

Inviscid Stability Theory for a Pair of Trailing Vortices near the Ground

Designations used in this Note correspond to those introduced by Crow.[12] The vortex wake is idealized as a pair of nearly parallel vortex lines located in plane $z = 0$ near the ground. The influence of the ground is modeled by a pair of inverted vortices located in plane $z = \mp 2h$. Inviscid theory predicts that the wake vortices will be traveled perpendicular to the runway with self-induced speed $u \sim \Gamma/4\pi h$ by the field of their image below the ground. The trailing vortices induct each other downward and approach the ground. This mean lateral vortex motion will be neglected in the stability analysis, and attention will be concentrated on development of vortex displacement from the unperturbed positions displayed. The validity of these geometric assumptions will be discussed later.

Because the vortex core size affects the results of the stability analysis rather weakly,[12,13] the simplest cutoff model is used here to avoid a singularity in the calculation of the self-induced velocity when $m = n$. Following Crow,[12] consider the sinusoidally deformed line vortices, so that ρ_m involving the location of vortex m becomes

$$\rho_m = \rho_m^o + \delta\rho_m, \qquad \delta\rho_m = (\eta_m^* e_y + \zeta_m^* e_z)\, e^{at + ikx_m} \tag{1}$$

It is assumed that

$$\frac{\delta\rho_m}{b} \ll 1, \qquad \left|\frac{\partial\delta\rho_m}{\partial x_m}\right| \ll 1 \tag{2}$$

In what follows, all quantities and functions are nondimensionalized with respect to the vortex separation b and a certain characteristic speed $U_0 = \Gamma/(2\pi b)$. In an inviscid fluid, a motion of elements of a vortex line satisfies the equation of fluid particles motion:

$$\frac{\partial\delta\rho_n}{\partial t} + \boldsymbol{U}_n\frac{\partial\delta\rho_n}{\partial x_n} = \delta\boldsymbol{U}_n \tag{3}$$

By substitution of Eqs. (1) and (2) and using Biot–Savart's law, Eq. (3) can be written in the form of a system of linear equations with unknown eigenvector $\boldsymbol{B}^* = (\eta_1^*, \eta_2^*, \zeta_1^*, \zeta_2^*)$:

$$(A + \alpha I)\boldsymbol{B}^* = 0 \tag{4}$$

(Ref. 17), where the $A = \{a_{ij}(H, \beta, \delta)\}$ coefficient matrix is presented in Ref. 17. Equations (4) have eigenvector solutions $\boldsymbol{B}^*$ only for four eigenvalues of α, which happen to be either purely real α_R or complex α_I with nonzero real part $Re(\alpha_I) \neq 0$. With increasing H, Eqs. (4) tend to equations obtained by Crow.[12] In the case $H = \infty$ the solution can be split into symmetric and antisymmetric modes. Only the symmetric mode involves strongly interacting long waves. It can be shown from Eqs. (4) that the interaction between the trailing vortices vanishes with decreasing $H \to 0$. Because it is not possible to split the solution of Eqs. (4) in the case of limited $H < \infty$ it contains both symmetric and antisymmetric modes. Figures 1–3 present the results obtained for different heights H. The value of $\delta/\beta = 0.063$ corresponds to that used by Crow.[12]

The eigenvalues $\alpha(\beta, \delta, H)$ are plotted against β in Fig. 1. The dotted curves represent positive values of $Re(\alpha_I)$, and the solid lines represent positive values of α_R. The six values of H were chosen to illustrate the point that $Re(\alpha)$ has one, two, or three local maxima along the β axis, depending on the value of height H. It was shown by Crow[12] that only one low-wave-number local maximum

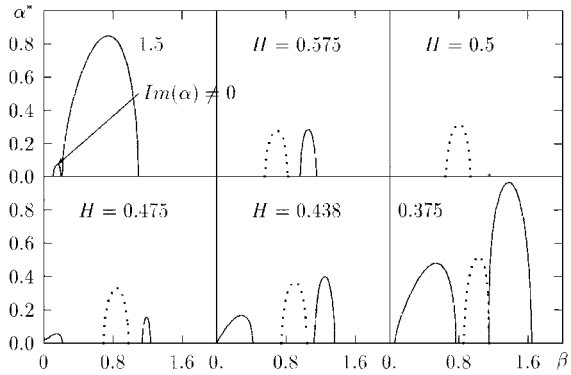

Fig. 1 Amplification rates $\alpha* = Re(\alpha) > 0$: $d = \delta/\beta = 0.063$; . . . , α_I and — —, α_R.

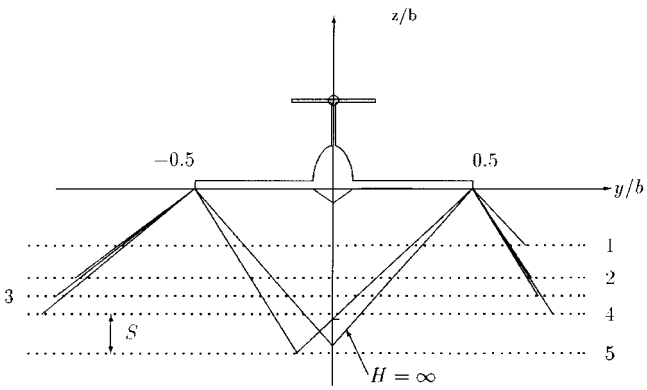

Fig. 2 Planes containing maximally unstable modes for different dimensionless heights. The dotted lines show different positions of the ground with respect to the aircraft: 1, $H = 0.2$; 2, $H = 0.313$; 3, $H = 0.375$; 4, $H = 0.438$; 5, $H = 0.575$; and S, region of the helical instability.

$\beta_{max} = 0.73$, $\alpha_{max} = 0.83$ is realized in the case $H = \infty$. It corresponds to the real eigenvalue α_R. The growing perturbations are planar symmetric waves, as sketched in Fig. 2. The planes containing any maximally unstable mode are inclined at about $\theta_1 = \theta_2 = 48$ deg, where $\tan\theta_i = \zeta_i^*/\eta_i^*$. The symmetry of the perturbation waves is violated with a decrease of the height H. The planes containing the planar sinusoidal waves are fixed at different angles θ_i to the horizontal. At $H = 0.575$, for example, the angle θ_1 is about 33 deg and θ_2 is about 42 deg, as can be seen directly from Fig. 2. The sinusoidal instability grows until the cores of the two vortices come into contact. Throughout the interval $0.575 \lesssim H \lesssim \infty$ the point of contact is located between the vortices below their unperturbed position. At $H = 0.575$, the point lies on the ground.

The second maximum, corresponding to the complex eigenvalue α_I, appears at $H \simeq 1.5$ in the region of the low wave numbers (Fig. 1). It is caused by interaction of the tip vortices with their mirror images. With a decrease of the height H, there takes place an increase of this maximum and its wave number β_{max}. The eigenmode associated with the positive $Re(\alpha_I)$ dominates throughout the interval $0.438 \lesssim H \lesssim 0.575$. There is the phase difference between the components of the eigenvector $B = (\eta_1^*, \eta_2^*, \zeta_1^*, \zeta_2^*)$, corresponding to α_I. The trailing vortices are bent into a helix. $Re(\alpha_I)$ associated with maximum of dependence $Re[\alpha_I(\beta)]$ is positive. Therefore the helix amplitude grows along the x axis, resulting in a helical instability.

The decrease of H shifts the maximum, corresponding to the real eigenvalue α_R, toward shorter wave numbers. At $H \simeq 0.5$, it vanishes, and then it appears again, and its magnitude grows with the decrease of the height H. The third maximum of the real eigenvalue appears at height $H \simeq 0.475$. The decrease of the height H results in the increase of the third maximum magnitude and its wave number (Fig. 1). The first real maximum dominates near the ground ($H \lesssim 0.438$), and the nature of the vortex instability depends completely on the interaction between the vortex and its mirror image. The mutual influence of the trailing vortices is weak. The growing perturbations are planar waves. Figure 2 shows that the planes are fixed at negative angles to the horizontal. The limiting value of this angle for $H \to 0$ is −42 deg. The instability of a trailing vortex in close proximity to the ground is like the so-called Crow instability[12] for two trailing vortices. In this case, the inverted vortex plays the role of the second trailing vortex. The instability grows until the vortex core comes into contact with the ground. The point of contact is located outside of the wingspan (Fig. 2). There is only one real maximum α_R at small height $H \lesssim 0.3$.

The maximum amplification rates are plotted against H in Fig. 3. With an increase of $H \to \infty$ the amplification rate α tends to 0.83. In very close proximity to the ground, $H \sim 0$, α is proportional to H^{-2}. The maximum, corresponding to the complex eigenvalue α_I, dominates throughout the interval $0.438 \lesssim H \lesssim 0.575$. The amplification rate is minimal in the region of the helical instability (Fig. 3). The dependence of the amplification rate on the vortex core size is rather weak.

It is found that the nature of the trailing vortex instability near the ground strongly depends on the dimensionless height H of the unperturbed vortex position. Three different types of the instability are illustrated schematically in Fig. 4. In the upper region, $H \gtrsim 0.575$, the instability is similar to Crow instability,[12] and the helical instability occurs in the middle region, $0.438 \lesssim H \lesssim 0.575$. The growing perturbations near the ground (lower region, $H < 0.438$) are planar waves, which are confined to fixed planes inclined at negative angles to the horizontal.

Turning now to validity of the geometric assumptions, we can conclude that the theory presented here is asymptotically correct at large height $H \to \infty$. The theory also is asymptotically correct in close vicinity to the ground, $H \to 0$, because here the interaction

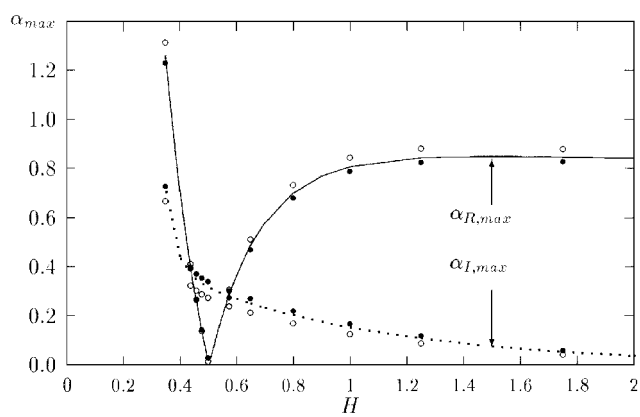

Fig. 3 Influence of the dimensionless height H on the maximum amplification rate: . . . , $\alpha_{I,max}$, $d = \delta/\beta = 0.063$; — —, $\alpha_{R,max}$, $d = 0.063$; ○ $d = 0.021$; and ● $d = 0.1$.

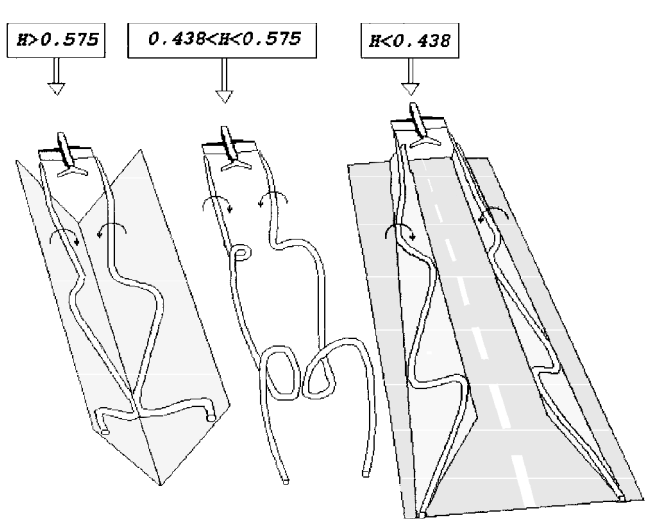

Fig. 4 Schematic of the vortex instability near the ground: 1, $H > 0.575$; 2, $0.575 > H > 0.438$; and 3, $H < 0.438$.

between the trailing vortices is very weak and the instability of each vortex can be regarded as the symmetrical Crow instability caused by mutual induction of the vortex and its mirror image. The mean lateral displacement of vortices is not important.

In the middle region of H, the vortex is inclined to the axis ox at the angles θ_y and θ_z, which may be estimated as

$$\theta_y \sim -\frac{\bar{\Gamma}}{2\pi A_R}\frac{4H^2}{1+4H^2}, \qquad \theta_z \sim \frac{\bar{\Gamma}}{4\pi H A_R}\frac{1}{1+4H^2}$$

where the circulation $\bar{\Gamma}$ is nondimensionalized with respect to the wing chord c. It can be shown that the angles θ_y and θ_z can be neglected throughout the interval $0.1 \leq H \leq 1.5$ for typical wings of aircraft. The underlying assumptions related to the geometry of the unperturbed vortices also are acceptable in the middle region. Consequently the theory presented is correct in inviscid fluid, at least qualitatively.

Conclusion

As follows from the presented linear analysis in inviscid fluid, the trailing vortices have undergone a growing sinusoidal instability in close vicinity to the ground and have come into contact with it. However, in reality the approaching vortices generate the boundary layer along the ground that separates and causes the primary vortices to follow a complicated trajectory. Our next paper will be devoted to the nonlinear instability of the trailing vortices in a viscous flow near the ground.

Acknowledgment

The authors would like to thank the Alexander von Humboldt Foundation for support of this work.

References

[1]Kornev, N. V., and Treshkov, V. K., "Numerical Investigation of Nonlinear Unsteady Aerodynamics of the WIG Vehicle," *Proceedings of the Intersociety High Performance Marine Vehicle Conference*, American Society of Naval Engineers, Arlington, VA, 1992, pp. ws38–ws48.

[2]Doligalski, T. L., Smith, C. R., and Walker, J. D. A., "Vortex Interactions with Walls," *Annual Review of Fluid Mechanics*, Vol. 26, 1994, pp. 573–616.

[3]Dee, F. W., and Nicholas, O. P., "Flight Measurements of Wing-Tip Vortex Motion near the Ground," Royal Aeronautical Establishment, CP-1065, London, Jan. 1968.

[4]Harvey, J. K., and Perry, F. J., "Flowfield Produced by Trailing Vortices in the Vicinity of the Ground," *AIAA Journal*, Vol. 9, No. 8, 1971, pp. 1659, 1660.

[5]Van Heijst, G. J. F., and Flor, J. B., *Mesoscale/Synoptic Coherent Structures in Geophysical Turbulence,* edited by J. C. J. Nihoul and B. M. Jouart, Elsevier, Amsterdam, 1989, pp. 591–608.

[6]Barker, S. J., and Crow, S. C., "The Motion of Two-Dimensional Vortex Pairs in Ground Effect," *Journal of Fluid Mechanics*, Vol. 82, Pt. 4, 1977, pp. 659–671.

[7]Ciffone, D. L., and Pedley, B., "Measured Wake–Vortex Characteristics of Aircraft in Ground Effect," *Journal of Aircraft*, Vol. 16, No. 2, 1979, pp. 102–109.

[8]Orlandi, P., "Vortex Dipole Rebound from a Wall," *Physics of Fluids A*, Vol. 2, No. 8, 1990, pp. 1429–1436.

[9]Robins, R. E., and Delisi, D. P., "Potential Hazard of Aircraft Wake Vortices in Ground Effect with Crosswind," *Journal of Aircraft*, Vol. 30, No. 2, 1993, pp. 201–206.

[10]Zheng, Z. C., and Ash, R. L., "Study of Aircraft Wake Vortex Behavior near the Ground," *AIAA Journal*, Vol. 34, No. 3, 1996, pp. 580–589.

[11]Teske, M. E., Bilanin, A. J., and Barry, J. W., "Decay of Aircraft Vortices near the Ground," *AIAA Journal*, Vol. 31, No. 8, 1993, pp. 1531–1533.

[12]Crow, S. C., "Stability Theory for a Pair of Trailing Vortices," *AIAA Journal*, Vol. 8, No. 12, 1970, pp. 2172–2179.

[13]Bliss, D., "Effect of Unsteady Forcing on the Sinusoidal Instability of Vortex Wakes," *Journal of Aircraft*, Vol. 19, No. 9, 1982, pp. 713–721.

[14]Crow, S. C., and Bate, E. R., "Lifespan of Trailing Vortices in a Turbulent Atmosphere," *Journal of Aircraft*, Vol. 13, No. 7, 1976, pp. 476–482.

[15]Green, G. C., "An Approximate Model of Vortex Decay in the Atmosphere," *Journal of Aircraft*, Vol. 23, No. 7, 1986, pp. 566–573.

[16]Liu, H.-T., "Effect of Ambient Turbulence on the Decay of a Trailing Vortex Wake," *Journal of Aircraft*, Vol. 29, No. 2, 1992, pp. 255–263.

[17]Kornev, N. V., "Instability and Nonlinear Dynamics of a Pair of Trailing Vortices in Ground Effect," *Mechanika Zhidkosti i Gaza*, No. 2, March–April 1997, pp. 103–109 (in Russian).

A. Plotkin
Associate Editor

Scaling Laws of Cylindrical Shells Under Lateral Pressure

A. Tabiei,* J. Sun,† and G. J. Simitses‡
University of Cincinnati, Cincinnati, Ohio 45221-0070

Introduction

BECAUSE of the complexity of the laminated composite structures and lack of complete design-based information, any new design must be extensively evaluated by experiments until it achieves the necessary reliability and safety. However, the experimental evaluation of these structures is costly and time consuming. More importantly, it is impractical to test large structures. Consequently, it is extremely useful if the behavior of a full-scale structure can be predicted from the behavior of a similar small-scale model.

Understanding the relationship between model and prototype behavior is essential in designing scaled-down models. To better understand the applicability of structural similitude in designing laminated composite structures, an analytical investigation was undertaken to assess the feasibility of its utility. Such a study is important because it provides the necessary scaling laws and scale factors that affect the accuracy of the predicted response.

Similitude theory has a wide application in solid, fluid, electrical, and thermal systems.[1] Structural similitude theory[2] is proven to be a very useful tool. In this theory, similarity is established in the solutions of the governing equations of the scaled-down model (scale model) and the full-scale structure (prototype).

The main objective of this study is to demonstrate the applicability of similitude theory in designing scaled-down models for predicting the buckling behavior of laminated cylindrical shells subjected to lateral pressure. Based on the resulting scaling laws, a new prediction equation is developed to establish the behavior of prototype both for complete and partial similarities.

Buckling Equations

Donnell-type equations governing buckling of laminated shells are commonly expressed in terms of variations of in-plane force and moment resultants, which can be subsequently expressed in terms of variations of displacements during buckling. The solution to the governing differential equations for laminated cross-ply shells with simply supported boundary conditions is straightforward. The result is a simple closed-form buckling criterion that is applicable for stress resultant N_{yy} due to lateral pressure (for details, see Ref. 3) as follows:

$$T_{33} + \frac{(2T_{12}T_{13}T_{23} - T_{11}T_{23}^2 - T_{22}T_{13}^2)}{(T_{11}T_{22} - T_{12}^2)} = -\bar{N}_{yy}\xi^2 \qquad (1)$$

where

$$\eta = \bar{m}\pi/L, \qquad \xi = \bar{n}/R$$

$$T_{11} = A_{11}\eta^2 + A_{66}\xi^2, \qquad T_{22} = A_{22}\xi^2 + A_{66}\eta^2$$

$$T_{12} = (A_{12} + A_{66})\xi\eta, \qquad T_{23} = A_{22}R^{-1}\xi$$

$$T_{13} = A_{12}R^{-1}\eta, \qquad T_{33} = D_{11}\eta^4 + 2\bar{D}_{12}\xi^2\eta^2 + D_{22}\xi^4 + A_{22}R^{-2} \qquad (2)$$

Received Oct. 16, 1996; revision received May 25, 1997; accepted for publication June 8, 1997.

*Assistant Professor, Department of Aerospace Engineering and Engineering Mechanics. Member AIAA.

†Graduate Research Assistant, Department of Aerospace Engineering and Engineering Mechanics.

‡Professor, Department of Aerospace Engineering and Engineering Mechanics. Fellow AIAA.